



Review article

Synthesis, characterization, computational, antioxidant and fluorescence properties of novel 1,3,5-trimesic hydrazones derivatives

Ibrahim Mhaidat^{*}, Fadel Alwedian, Taher Ababneh, Ayman Shdefat, Hasan Tashtoush

Department of Chemistry, Faculty of Science, Yarmouk University, Irbid, 1163, Jordan

ARTICLE INFO

Keywords:

Trimesic acid
Hydrazones
Antioxidant
Spectrophotometric
Fluorescence
DFT

ABSTRACT

New photophysical and antioxidant materials of trimesic trihydrazide derivatives were synthesized by one-pot stage of trimesic trihydrazide and different aromatic aldehydes. All compounds were characterized by spectroscopic techniques (NMR, MS, and IR) and elemental analysis. The absorption and emission spectral characteristics of hydrazone derivatives were investigated. The absorption maxima showed red shift relative to the starting compound. While the emission maxima showed clear dependent on the type of substituents. The electron donating and electron withdrawing showed red and blue shifts relative to the starting compound, respectively. The compounds' effectiveness as antioxidant was estimated by DPPH radical scavenging and ABTS radical cation assays in vitro which indicated that the derivatives could be used as potential antioxidants. In addition, compounds 3g, and 3i showed strong antioxidant activities according to the DPPH assay and compounds 3c and 3m exhibited good antioxidant activities in ABTS assay. Antimicrobial activity of the derivatives was estimated using a micro-broth dilution method. Furthermore, molecular geometries of all prepared derivatives were fully optimized using density functional theory (DFT) calculations at the 6-31G(d)/B3LYP level of theory.

1. Introduction

Hydrazones are a special class of Schiff bases with a general structure $R_1R_2C = NNH_2$ [1, 2]. Their structures contain both electron-donating and electron-withdrawing substituents and are basically related to ketones and aldehydes [3]. The combination of hydrazones with other functional groups leads to a compound with uniquely physical and chemical characteristics which are greatly affecting their biological and pharmacological properties.

Hydrazones are commonly used as biologically active reagents to treat several diseases including anti-microbial [4] anti-tumor [5, 6], tuberculosis [6], leprosy and mental disorder [7]. In addition, they were used as herbicides, insecticides, nematocides, rodenticides and plant growth regulators [8]. Antioxidants are responsible for the defense mechanisms of organisms against pathologies associated with the attack of free radicals that can be produced by the oxidation reactions, which in turn, can initiate chain reactions. It is well established that free radical chain reaction in the cell may cause its damage or death. Antioxidants terminate these chain reactions by removing free radical intermediates and inhibit other oxidative reactions [9, 10, 11, 12]. Experimentally, arylhydrazone compounds can function as free-radical scavengers [13, 14] and as antioxidant agents [15, 16, 17].

The aryl substitution pattern of hydrazones produced a unique structure of arylhydrazone. This structure is greatly affecting both luminescence efficiency and photophysical properties of hydrazones [18]. A wide range of triazine and hydrazone-containing molecules has been studied using DFT methods. Computational analysis is carried out to confirm the experimental findings and to investigate further structural features [19, 20, 21].

The present work aims to synthesis and characterization of a new substituted arylhydrazones derived from trimesic acid. Their molecular structures were identified using elemental analysis, 1H -NMR, ^{13}C -NMR, FT-IR, and UV-vis spectroscopy, and further confirmed by DFT computational study. The antioxidant and biological activities of the synthesized molecules were also investigated.

2. Results and discussion

2.1. Synthesis and characterization of trimesic hydrazones (3a-3m)

The synthetic routes of the trimesic hydrazone (3a-3m) are summarized in Figure 1. Hydrazone compounds were synthesized as specified by two reactions: methyl trimesic ester reacts with hydrazine hydrates to

* Corresponding author.

E-mail address: ibrahim.m@yu.edu.jo (I. Mhaidat).

yield trimesic trihydrazide followed by a condensation reaction with aromatic aldehydes. The process provided excellent yields (85–95%). The IUPAC names, yields, melting points, elemental analysis of (C, H and N), IR and NMR are summarized in the experimental part. The Infrared spectra of the synthesized compounds reveal the bands at 3187–3271, 1649–1671, 1512–1591 cm^{-1} which are corresponding to the stretching frequencies of NH, C=O and C=N functional groups of trimesic hydrazine compounds, respectively. In addition to that, other characteristic bands at 3394 and 3441 cm^{-1} assigned to ν (OH) for **3d** and **3m**, respectively, and a band at 2360 cm^{-1} due to ν (C≡N) for **3j**. The $^1\text{H-NMR}$ spectra of **3a-3m** compounds show a singlet peak at 8.3–8.9 ppm of azomethine protons ($-\text{CH} = \text{N}-$) and a singlet band at 11.85–12.75 ppm of imino protons ($-\text{NH}$). Moreover, the aromatic protons appear on the aromatic regions. Similarly, the $^{13}\text{C-NMR}$ spectra for all compounds show peaks at 161.0 to 163.0 and 142.0–146.0 ppm for carbonyl (C=O) and imine (C=N) groups, respectively. Moreover, the spectra of **3d**, **3f**, and **3i** show peaks in the range of 55.0–57.0 ppm due to the presence of methoxy group; **3c** exhibits a peak at 39.7 ppm for alkyl amine; **3h** and **3i** display several peaks in the range of 16.0–24.0 ppm due to the presence of alkyl groups. The aromatic carbons appeared in the expected aromatic regions.

2.2. Biological activity

2.2.1. Antimicrobial properties

All synthesized compounds were screened as a potential antimicrobial agent. Their antimicrobial activities were tested in vitro against Gram positive bacteria and Gram negative bacteria, including (*Escherichia coli*; *Klebsiella pneumoniae*; *Proteus mirabilis*; *Salmonella enteritidis*, *Pseudomonas aeruginosa*; *Staphylococcus aureus*; *Enterococcus faecalis*; *Bacillus cereus*). Unfortunately, all these compounds were inactive against all tested bacteria used in this study. The range of concentrations was in

range from 500 to 0.5 $\mu\text{g/mL}$ of the respective compounds under investigation with positive and negative control well. Amoxicillin and DMSO were used as positive and negative controls. The MIC of all tested chemicals were above 500 $\mu\text{g/mL}$ and considered inactive.

2.2.2. Scavenging radical activity on 2,2-diphenyl-1-picrylhydrazyl (DPPH) radical

Compound **3i** (with a methoxy and two methyl groups on phenyl) and compound **3g** (with a Cl group in the ortho-position of phenyl) showed the best inhibitory activities with 0.12 and 0.6 $\mu\text{g/mL}$ IC_{50} values, respectively. The **3i** and **3g** had higher antioxidant activities than the ascorbic acid with 1.3 $\mu\text{g/mL}$ IC_{50} value. Compounds **3a** with the thiophene ring and **3f** with the three methoxy groups in positions 2,4, and 5 of phenyl showed strong antioxidant activities with the 14.0 and 17.0 $\mu\text{g/mL}$ IC_{50} values, respectively; however, these compounds showed lower activities relative to the ascorbic acid. Compounds **3b**, **3j**, and **3k** exhibited moderately antioxidant activities with 70, 53, and 53 $\mu\text{g/mL}$ IC_{50} values, respectively. Compounds **3d**, **3e**, and **3h** showed weak antioxidant activities with 610, 140 and 800 $\mu\text{g/mL}$ IC_{50} values, respectively. While compounds **3c**, **3l** and **3m** did not show any antioxidant properties, see [Table 1](#) and [Figure 2](#).

2.2.3. Scavenging radical activity on 2,2'-azinobis(3-ethylbenzthiazoline-6-sulfonic acid) (ABTS $^{+\cdot}$) radical cation

Compounds **3a-3m** established strong to moderately antioxidant activity with 13–41 $\mu\text{g/mL}$ IC_{50} values in ABTS assay. Compound **3c** with a N,N-dimethylamino group in the para-position of phenyl and **3m** with a hydroxy group of naphthyl had the most antioxidant behavior among the tested compounds in ABTS assay with the 13 and 14 $\mu\text{g/mL}$ IC_{50} values, respectively. Compounds **3d**, **3j**, **3f**, **3b**, **3e**, **3g**, **3a**, **2l**, and **3i** indicated good ABTS $^{+\cdot}$ radical scavenging activities with 17, 19, 23, 26, 27,

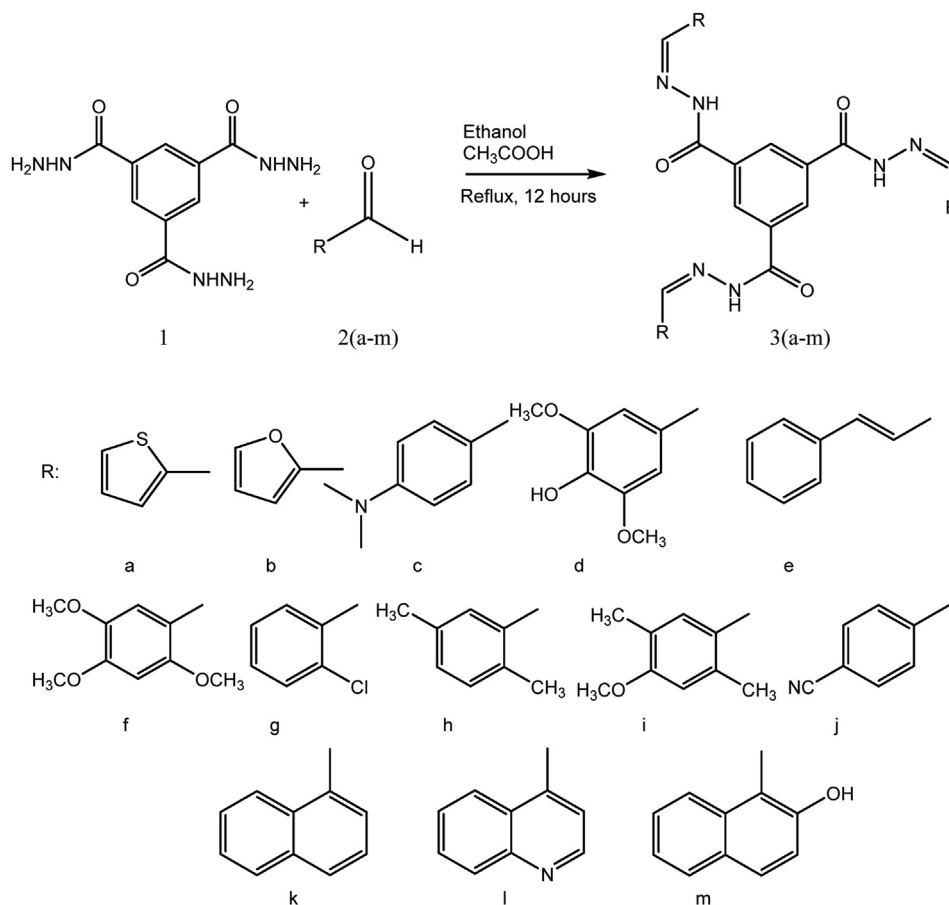


Figure 1. The synthetic route for trimesic hydrazones (**3a-3m**).

27, 28, 28, and 29 $\mu\text{g/mL}$ IC_{50} values, respectively. On the other hand, compounds 3k and 3h showed moderately activities with 35 and 41 $\mu\text{g/mL}$ IC_{50} values, respectively. All the compounds exhibited lower antioxidant activities compared to the ascorbic acid, see Table 1 and Figure 3.

The antioxidant results did not provide any direct relationship between the position and the type of substituents on aromatic ring and the antioxidant activity of all tested compounds, some authors reported similar finding [22, 23, 24, 25, 26, 27].

2.3. The spectrophotometric and fluorometric measurements

The Ultraviolet-visible spectra of the compounds 3a-3m were measured in DMSO. Figure 4 shows the UV spectra of selected compounds (3b, 3c, 3f, 3g, 3i, 3j, 3k and 3l), with the corresponding maximum wavelengths of new compounds 3a-3m recorded in Table 2. The UV-vis spectra of all compounds exhibited λ_{max} between 295–366 nm, which is attributed to π to π^* transitions. Also, it was observed that compounds with electron-donating substituents such as amino group ($-\text{N}(\text{CH}_3)_2$), exhibited longer maximum wavelengths. On the other hand, compounds with electron-withdrawing substituents had shorter maximum wavelengths.

The normalized fluorescence spectra of all compounds were recorded under similar conditions using DMSO as solvent, see Figures 5 and 6. The maximum emission wavelengths for all compounds are listed in Table 2. The effect of substituents on the emission maxima are divided into three groups. The aromatic ring substituent on compounds 3h and 3k show no significant influence on the fluorescence properties. Compounds 3a, 3c, 3d, 3e, and 3m show red shifts relative to the starting compound. This may be correlated with influence of electron-donating groups. On the other hand, compounds 3b, 3f, 3g, 3j and 3l showed blue shifts by about 25 nm, which may be correlated to presence of electron-withdrawing groups. These results were in good agreement with other published studies [18, 23].

2.4. Computational study

We have undertaken an intensive theoretical investigation in order to find the most-stable minimal-energy structure for each derivative. The methodology considers all initial molecular orientations at the semi-empirical/PM6 quantum chemical level by running a conformer distribution calculation. After exploring all possible conformers with such flexible molecules, the search is narrowed down and a higher DFT level of theory is applied to finally obtain the optimized structures. The absence of imaginary frequencies in the vibrational mode calculation confirmed true minima on the potential energy surface for each derivative. The optimized ground-state geometries of derivatives (3a-3m) at the B3LYP/

Table 1. Antioxidant activity results of synthesized compounds 3a-3m.

Compound	IC_{50} ($\mu\text{g/mL}$) DPPH	IC_{50} ($\mu\text{g/mL}$) ABTS
3a	15	28
3b	70	26
3c	NA	13
3d	610	17
3e	140	27
3f	17	23
3g	0.6	27
3h	800	41
3i	0.12	29
3j	53	19
3k	53	35
3l	NA	28
3m	NA	14
Ascorbic acid	1.3	2

6-31G(d) level of theory are depicted in Figure 7. All structures feature trimeric propeller-shaped arrangements around a central moiety of 1,3,5-trisubstituted benzene. To get a better insight into the extent of spatial twist exhibited by each of the three aryl moieties in reference to the central trisubstituted arene backbone, the angles between the central benzene plane and cyclic aryl substituents were calculated. For each tripodal molecule, the three dihedral angles and their average are listed in Table 3. Average values ranged from 18.18° to 53.39°. While compounds 3a-3j (all monocyclic aryl side groups) show relatively small variation in average dihedral angles among them, compounds 3k, 3l and 3m (all bicyclic aryl side groups) have noticeably higher values 40.83°, 38.98° and 53.39°, respectively. This reflects the direct impact of structure on orientation of substituents. The closest compound to a planar geometry is 3b with an average dihedral angle of 18.18°. On the other hand, compound 3m has the largest average dihedral angle 53.39°, which could be attributed to steric requirements as well as being the only compound with the presence of H-bonding between adjacent substituents (H-bond lengths (Å) are shown in Figure 6. Notice that compound 3d also features H-bonding, but it is within the same substituent, between a phenolic hydrogen and methoxy oxygen (phO-H...O-Me). The results are comparable to trimer structures reported elsewhere [28]. This class of molecules containing aromatic dimer and trimer side groups is of great interest in biological systems. For instance, aromatic trimer-containing molecules are present in several proteins and are considered the building blocks for higher-order clusters [29, 30]. Therefore, it may be of interest for future research to investigate this series of compounds and expand it to other aromatic side groups found in proteins with the potential of biological activity and as promising building units for new assemblies.

3. Materials and methods

Solvents and chemical compounds such as methanol, ethanol, DMF, DMSO, diethyl ether, ethyl acetate, hexane, chloroform and trimesic acid were supplied from Sigma Aldrich and Fluka and were used as received without any further purification unless mentioned.

Melting points were tested on an electrothermal-digital apparatus. Nuclear magnetic resonance (NMR) spectra were determined using a Bruker 400 MHz (for ^1H) and 100 MHz (for ^{13}C) Avance III spectrometer. The infrared spectral data were detected on Bruker alpha FTIR. The elemental analyses of the elements (C, H and N) were carried out on Euro EA elemental analyzer 300.

3.1. Preparation of trimesic hydrazide hydrazone (3a-3m)

A mixture of 1.0 mmol (0.25 g) of trimesic trihydrazide (1) and 3.0 mmol of aromatic aldehydes (2a-2m) in 15 mL ethanol was refluxed for 12 h with catalytic amount of glacial acetic acid, Figure 1. The mixture was cooled then the precipitate was collected and recrystallized from DMF/H₂O [27].

Tris(thiophen-2-ylmethylene)benzene-1,3,5-tricarbohydrazide (3a)

White powder, yield = 92%, mp: dc > 250 °C, IR spectrum (νcm^{-1}): 3236 (NH), 1659 (Amide carbonyl group, C=O), 1512 (C=N). $^1\text{H-NMR}$ (d^6 -DMSO), (δ ppm): 7.16–7.18 (t, 3H (J = 4.30 Hz), Aromatic), 7.52–7.53 (d, 3H (J = 2.96Hz), Aromatic), 7.72–7.73 (d, 3H (J = 5.01Hz), Aromatic), 8.60 (s, 3H, N=CH), 8.70 (s, 3H, Aromatic), 12.16 (s, 3H, NH). $^{13}\text{C-NMR}$ (d^6 -DMSO) spectrum, (δ ppm): 127.9, 129.2, 129.7, 131.4, 134.0, 138.7, 143.6, 161.7. Elemental Analysis C₂₄H₁₈N₆O₃S₃ (534.63) (%) found C 53.06; H 3.73; N 15.46, calculated C 53.92; H 3.39; N 15.72.

Tris(furan-2-ylmethylene)benzene-1,3,5-tricarbohydrazide (3b)

White powder, yield = 94%, mp: 246–248 °C, IR spectrum (νcm^{-1}): 3205 (NH), 1650 (Amide carbonyl group, C=O), 1513 (C=N). $^1\text{H-NMR}$ (d^6 -DMSO) spectrum (δ ppm): 6.67–6.68 (t, 3H (J = 5.04Hz), Aromatic), 6.99–7.00 (d, 3H (J = 3.28Hz), Aromatic), 7.89 (s, 3H, Aromatic), 8.38 (s, 3H, N=CH), 8.62 (s, 3H, Aromatic), 12.1 (s, 3H, NH). $^{13}\text{C-NMR}$ (d^6 -DMSO) spectrum, (δ ppm): 112.7, 114.6, 130.2, 134.5, 138.6, 145.9,

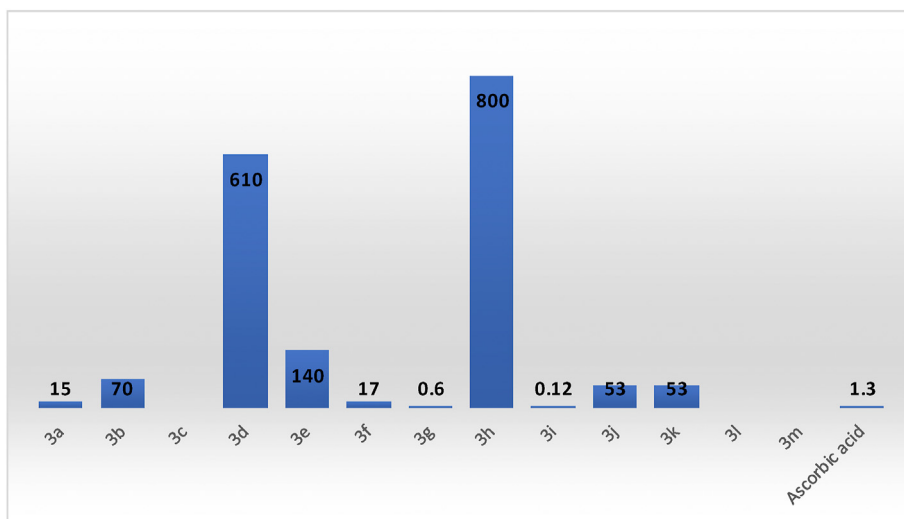


Figure 2. IC₅₀ (µg/mL) values (concentration needed for reducing DPPH absorption by 50% at 517 nm) of compounds 3a,3b,3e, 3f, 3g, 3i, 3j, 3k, and ascorbic acid. No data for 3c, 3l and 3m in DPPH assay were presented due to lack of activity.

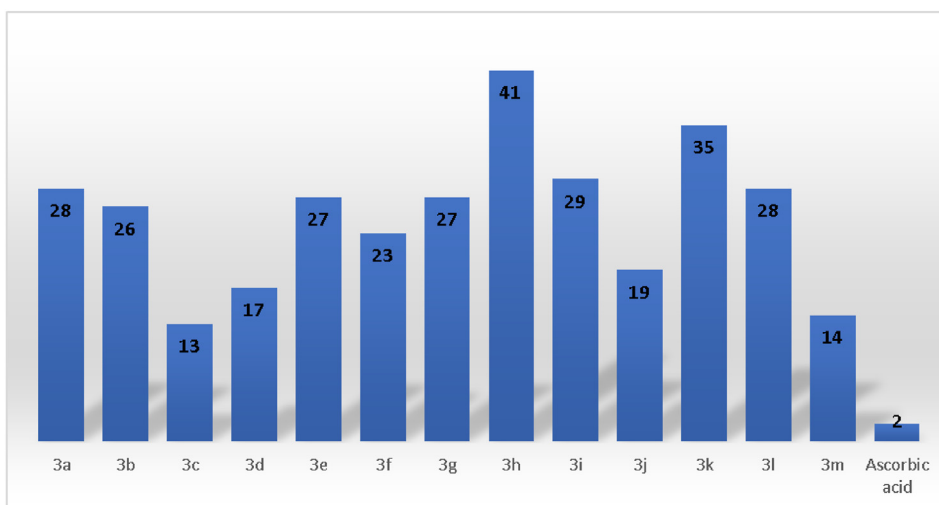


Figure 3. IC₅₀ (µg/mL) values (concentration needed for reducing ABTS^{•+} absorption by 50% at 734 nm) of compounds 3a-3m ascorbic acid.

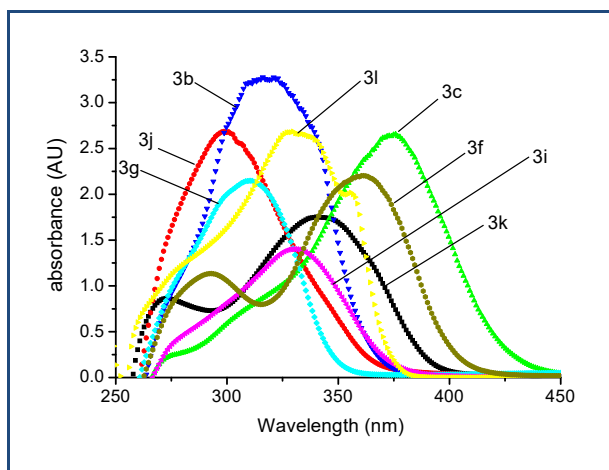


Figure 4. The UV-vis spectra for the hydrazones (3b, 3c, 3f, 3g, 3i, 3j, 3k and 3l) in DMSO at a room temperature.

149.7, 162.6. Elemental Analysis C₂₄H₁₈N₆O₆ (486.44) (%) found C 59.14; H 3.90; N 17.34. calculated C 59.26; H 3.73; N 17.28.

Tris(4-(dimethylamino)benzylidene)benzene-1,3,5-tricarbohydrazide (3c)

Yellow powder, yield = 91%, mp: dc > 250 °C. IR spectrum (ν cm⁻¹): 3212 (NH), 1651 (Amide carbonyl group, C=O), 1589 (C=N). ¹H-NMR (d⁶-DMSO) spectrum (δ ppm): 2.99 (s, 18H, N-(CH₃)₂), 6.77–6.79 (d, 6H(J = 8.92Hz), Aromatic), 7.57–7.59 (d, 6H(J = 8.85Hz), Aromatic), 8.36 (s, 3H, N=CH), 8.58 (s, 3H, Aromatic), 11.88 (s, 3H, NH). ¹³C-

Table 2. The maximum wavelengths of absorption and emission of compounds 3a-3m.

Compound	λ_{abs} (nm)	λ_{em} (nm)	Compound	λ_{abs} (nm)	λ_{em} (nm)
3a	325	480	3h	310	430
3b	320	400	3i	330	465
3c	370	516	3j	295	404
3d	330	450	3k	340	430
3e	335	460	3l	330	405
3f	360	422	3m	335	440
3g	310	402			

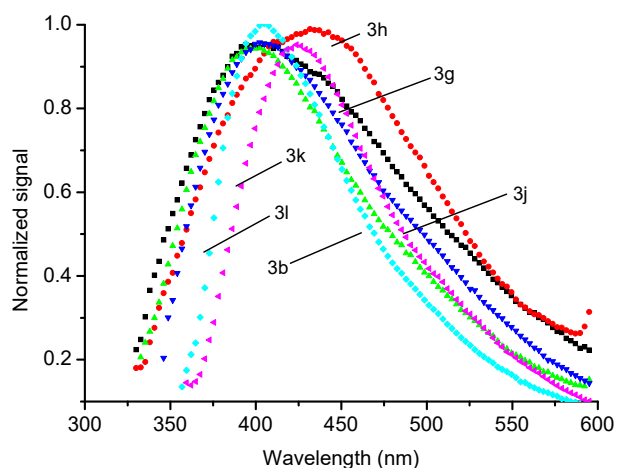


Figure 5. The normalized fluorescence spectra of (3b,3g, 3h, 3j, 3k, and 3l) in DMSO at room temperature.

NMR(d^6 -DMSO) spectrum (δ ppm): 39.7, 111.7, 121.3, 128.5, 129.3, 134.3, 149.2, 151.6, 161.1. Elemental Analysis $C_{36}H_{39}N_9O_3$ (645.75) (%) found C 66.21; H 6.52; N 18.60. calculated C 66.96; H 6.09; N 19.52.

Tris(4-hydroxy-3,5-dimethoxybenzylidene)benzene-1,3,5-tricarbohydrazide (3d)

Green powder, yield = 89%, mp: dc > 250 °C. IR spectrum (ν cm^{-1}): 3394(OH), 3251 (NH), 1650 (Amide carbonyl group, C=O), 1556 (C=N). 1H -NMR(d^6 -DMSO) spectrum (δ ppm): 3.84 (s, 18H, OCH₃), 7.01 (s, 6H, Aromatic), 8.36 (s, 3H, N=CH), 8.55 (s, 3H, Aromatic), 8.99 (s, 3H, OH), 12.08 (s, 3H, NH). ^{13}C -NMR(d^6 -DMSO) spectrum (δ ppm): 56.0, 104.7, 124.2, 129.6, 134.2, 138.1, 148.1, 149.2, 161.9. Elemental Analysis $C_{36}H_{36}N_6O_{12}$ (744.7) (%) found C 57.91; H 4.95; N 11.20. calculated C 58.06; H 4.87; N 11.29.

Tris(E)-3-phenylallylidene)benzene-1,3,5-tricarbohydrazide (3e)

White powder, yield = 93%, mp: 218–220 °C. IR spectrum (ν cm^{-1}): 3215 (NH), 1651 (Amide carbonyl group, C=O), 1543 (C=N). 1H -NMR(d^6 -DMSO) spectrum (δ ppm): 7.11–7.13 (d, 6H(J = 6.36Hz), Aromatic), 7.35–7.43 (m, 9H, Aromatic), 7.65–7.67 (d, 6H(J = 7.35Hz), HC = CH), 8.29–8.31 (d, 3H(J = 7.60Hz), N=CH), 8.64 (s, 3H, Aromatic), 12.10 (s, 3H, NH). ^{13}C -NMR(d^6 -DMSO) spectrum (δ ppm): 125.5, 127.1, 128.8, 128.9, 129.8, 134.0, 135.8, 139.5, 150.5, 161.78. Elemental Analysis $C_{36}H_{30}N_6O_3$ (594.66) (%) found C 71.97; H 5.45; N 14.70. calculated C 72.71; H 5.08; N 14.13.

Tris(2,4,5-trimethoxybenzylidene)benzene-1,3,5-tricarbohydrazide (3f)

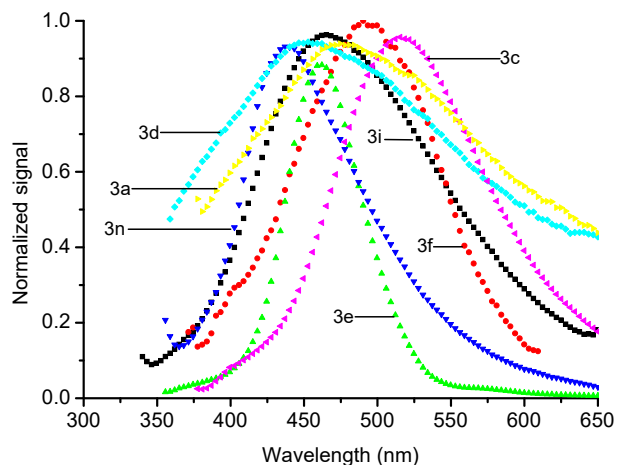


Figure 6. The normalized fluorescence spectra of (3a, 3c, 3d, 3e, 3i, 3f, and 3m) in DMSO at room temperature.

White powder, yield = 93%, mp: dc > 250 °C. IR spectrum (ν cm^{-1}): 3210 (NH), 1651 (Amide carbonyl group, C=O), 1556 (C=N). 1H -NMR(d^6 -DMSO) spectrum (δ ppm): 3.79 (s, 9H, OCH₃), 3.87 (s, 9H, OCH₃), 3.89 (s, 9H, OCH₃), 6.72 (s, 3H, Aromatic), 7.31 (s, 3H, Aromatic), 8.61 (s, 3H, N=CH), 8.79 (s, 3H, Aromatic), 12.00 (s, 3H, NH). ^{13}C -NMR(d^6 -DMSO) spectrum (δ ppm): 56.2, 56.4, 57.0, 98.3, 108.0, 113.7, 130.0, 134.6, 143.7, 144.4, 152.7, 154.0, 162.1. Elemental Analysis $C_{39}H_{42}N_6O_{12}$ (786.78) (%) found C 58.80; H 5.72; N 11.60. calculated C 59.54; H 5.38; N 10.68.

Tris(2-chlorobenzylidene)benzene-1,3,5-tricarbohydrazide (3g)

White powder, yield = 88%, mp: dc > 250 °C. IR spectrum (ν cm^{-1}): 3215 (NH), 1652 (Amide carbonyl group, C=O), 1558 (C=N). 1H -NMR(d^6 -DMSO) spectrum (δ ppm): 7.47–7.58 (m, 9H, Aromatic), 8.07–8.09 (d, 3H(J = 9.28z), Aromatic), 8.73 (s, 3H, N=CH), 8.94 (s, 3H, Aromatic), 12.40 (s, 3H, NH). ^{13}C -NMR(d^6 -DMSO) spectrum (δ ppm): 126.9, 127.6, 129.9, 130.0, 131.3, 131.7, 133.3, 133.9, 144.5, 161.9. Elemental Analysis $C_{30}H_{21}Cl_3N_6O_3$ (619.89) (%) found C 57.87; H 5.61; N 10.83. calculated C, 58.13; H 5.38; N, 10.68.

Tris(2,5-dimethylbenzylidene)benzene-1,3,5-tricarbohydrazide (3h)

White powder, yield = 85%, mp: dc > 250 °C. IR spectrum (ν cm^{-1}): 3220 (NH), 1668 (Amide carbonyl group, C=O), 1556 (C=N). 1H -NMR(d^6 -DMSO) spectrum (δ ppm): 2.33 (s, 9H, CH₃), 2.42 (s, 9H, CH₃), 7.17 (s, 6H, Aromatic), 7.73 (s, 3H, Aromatic), 8.66 (s, 3H, N=CH), 8.78 (s, 3H, Aromatic), 12.16 (s, 3H, NH). ^{13}C -NMR(d^6 -DMSO) spectrum (δ ppm): 18.1, 24.3, 126.5, 128.5, 129.1, 129.4, 131.4, 134.7, 136.7, 137.8, 143.0, 162.3. Elemental Analysis $C_{36}H_{36}N_6O_3$ (600.71) (%) found C 71.52; H 5.95; N 14.14. calculated C, 71.98; H, 6.04; N, 13.99.

Tris(4-methoxy-2,5-dimethylbenzylidene)benzene-1,3,5-tricarbohydrazide (3i)

White powder, yield = 91%, mp: dc > 250 °C. IR spectrum (ν cm^{-1}): 3187 (NH), 1660 (Amide carbonyl group, C=O), 1591 (C=N). 1H -NMR(d^6 -DMSO) spectrum (δ ppm): 2.16 (s, 9H, CH₃), 2.43 (s, 9H, CH₃), 3.83 (s, 9H, OCH₃), 6.84 (s, 3H, Aromatic), 7.70 (s, 3H, Aromatic), 8.60 (s, 3H, N=CH), 8.72 (s, 3H, Aromatic), 12.03 (s, 3H, NH). ^{13}C -NMR(d^6 -DMSO) spectrum (δ ppm): 16.0, 19.2, 55.8, 112.8, 124.1, 128.2, 129.9, 131.1, 134.7, 137.2, 147.5, 159.2, 162.1. Elemental Analysis $C_{39}H_{42}N_6O_6$ (690.79) (%) found C 66.95; H 6.78; N 12.79. calculated C 67.81; H 6.13; N 12.17.

Tris(4-cyanobenzylidene)benzene-1,3,5-tricarbohydrazide (3j)

Yellow powder, yield = 90%, mp: dc > 250 °C. IR spectrum (ν cm^{-1}): 3210 (NH), 2360 (C≡N), 1665 (Amide carbonyl group, C=O), 1555 (C=N). 1H -NMR(d^6 -DMSO) spectrum (δ ppm): 7.96 (s, 12H, Aromatic), 8.56 (s, 3H, N=CH), 8.70 (s, 3H, Aromatic), 12.47 (s, 3H, NH). ^{13}C -NMR(d^6 -DMSO) spectrum (δ ppm): 112.0, 118.6, 127.7, 130.2, 132.7, 133.8, 138.5, 146.6, 162.2. Elemental Analysis $C_{33}H_{21}N_9O_3$ (591.58) (%) found C 65.98; H 4.01; N 20.78. calculated C 67.00; H 3.58; N 21.31.

Tris(naphthalen-1-ylmethylene)benzene-1,3,5-tricarbohydrazide (3k)

Yellow powder, yield = 88%, mp: dc > 250 °C. IR spectrum (ν cm^{-1}): 3187 (NH), 1658 (Amide carbonyl group, C=O), 1578 (C=N). 1H -NMR(d^6 -DMSO) spectrum (δ ppm): 7.63–7.72 (m, 12H, Aromatic), 8.01–8.09 (m, 6H, Aromatic), 8.80 (s, 3H, N=CH), 8.87–8.89 (d, 3H(J = 8.60Hz), Aromatic), 9.22 (s, 3H, Aromatic), 12.36 (s, 3H, NH). ^{13}C -NMR(d^6 -DMSO) spectrum (δ ppm): 126.1, 126.8, 127.7, 127.9, 128.3, 129.3, 129.8, 130.3, 130.8, 130.7, 131.2, 134.7, 148.8, 162.4. Elemental Analysis $C_{42}H_{30}N_6O_3$ (666.73) (%) found C 75.23; H 4.31; N 12.44. calculated C 75.66; H 4.54; N, 12.60.

Tris(quinolin-4-ylmethylene)benzene-1,3,5-tricarbohydrazide (3l)

White powder, yield = 87%, mp: 239–241 °C. IR spectrum (ν cm^{-1}): 3234 (NH), 1671 (Amide carbonyl group, C=O), 1559 (C=N). 1H -NMR(d^6 -DMSO) spectrum (δ ppm): 7.77–7.81 (t, 3H(J = 7.31Hz), Aromatic), 7.85–7.89 (t, 3H(J = 7.45Hz), Aromatic), 7.92–7.93 (d, 3H(J = 3.92Hz), Aromatic), 8.13–8.15 (d, 3H(J = 8.2Hz), Aromatic), 8.79–8.77 (d, 3H(J = 8.36Hz), Aromatic), 8.84 (s, 3H, N=CH), 9.03–9.04 (d, 3H(J = 3.99Hz), Aromatic), 9.21 (s, 3H, Aromatic), 12.64 (s, 3H, NH). ^{13}C -NMR(d^6 -DMSO) spectrum (δ ppm): 120.5, 125.1, 128.2, 130.2, 130.3, 130.6, 130.8, 134.5, 137.6, 146.3, 148.9, 150.9, 162.6. Elemental

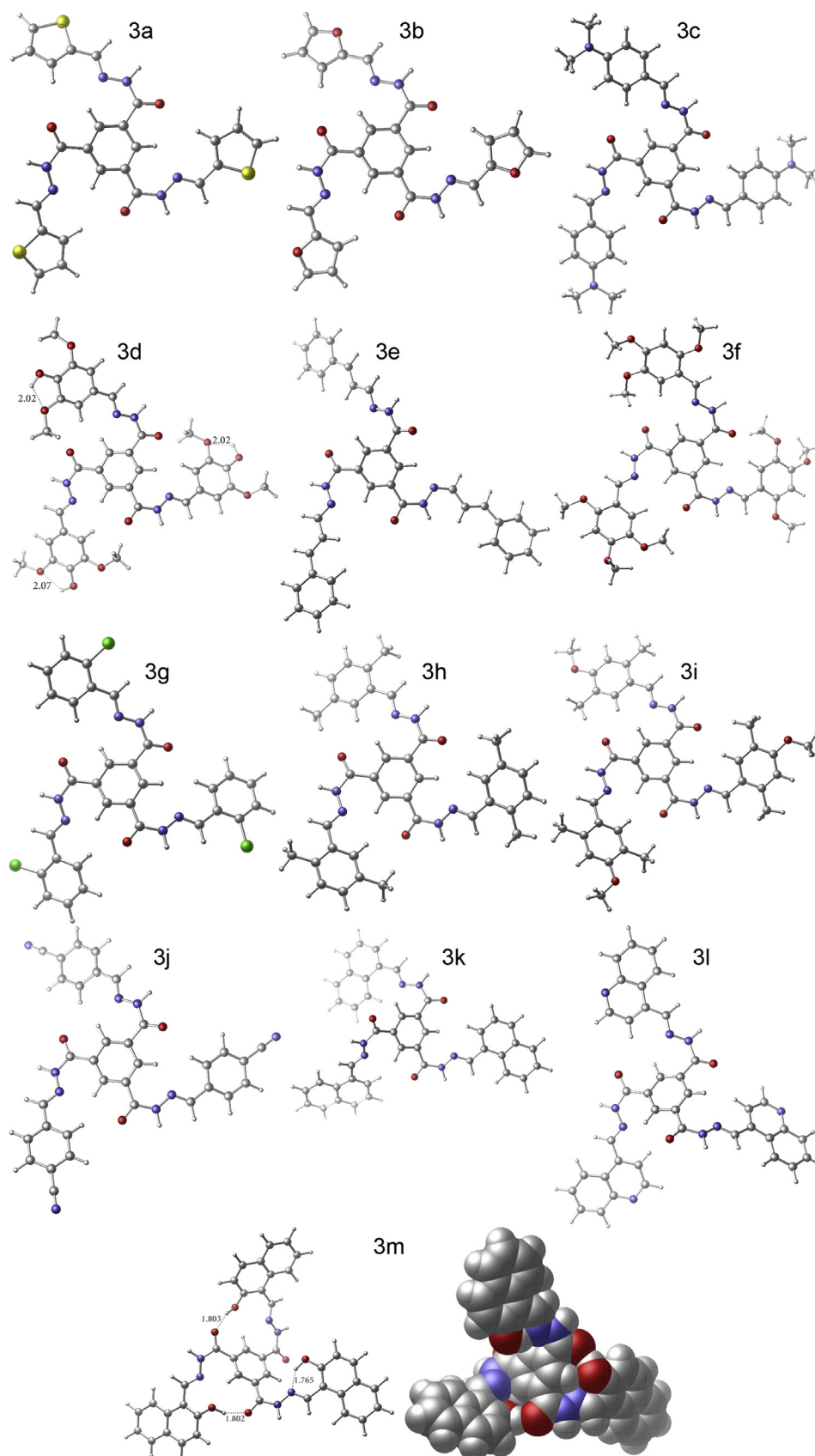


Figure 7. The optimized ground-state geometries of 3a-3 m at the 6-31G(d)/B3LYP level of theory (structure of 3m is also depicted in space-filling view showing propeller shape).

Table 3. Dihedral angles (°) between central benzene ring plane and aryl substituents of **3a-3m**.

Compound	Dihedral angles			Average
3a	18.34	12.56	24.90	18.60
3b	16.62	14.20	23.71	18.18
3c	16.27	25.19	19.93	20.46
3d	31.31	27.77	22.06	27.05
3e	30.70	28.86	35.27	31.61
3f	26.37	27.63	15.79	23.26
3g	26.45	30.96	20.00	25.80
3h	20.81	24.84	25.63	23.76
3i	23.43	18.42	23.95	21.93
3j	19.30	22.63	27.95	23.29
3k	42.25	36.75	43.50	40.83
3l	38.00	39.13	39.82	38.98
3m	44.68	59.86	55.64	53.39

Analysis C₃₉H₂₇N₉O₃ (669.69) (%) found C 69.84; H 3.97; N 18.73. calculated C 69.95; H 4.06; N 18.82.

Tris(2-hydroxynaphthalen-1-yl)methylenebenzene-1,3,5-tricarbohy-drazide (3m) [31]

Yellow powder, yield = 89%, mp: 245–246 °C, IR spectrum (ν cm⁻¹): 3441 (OH), 3213 (NH), 1649 (Amide carbonyl group, C=O), 1573 (C=N). ¹H-NMR (d⁶-DMSO) spectrum (δ ppm): 7.26–7.29 (d, 3H(J = 8.96Hz), Aromatic), 7.42–7.45 (t, 3H(J = 7.34Hz), Aromatic), 7.63–7.65 (t, 3H(J = 7.64Hz), Aromatic), 7.92–7.94 (d, 3H(J = 7.92Hz), Aromatic), 7.97–7.99 (d, 3H(J = 8.96Hz), Aromatic), 8.32–8.34 (d, 3H(J = 6.17Hz), Aromatic), 8.87 (s, 3H, N=CH), 9.59 (s, 3H, Aromatic), 12.64 (s, 3H, OH), 12.72 (s, 3H, NH). ¹³C-NMR(d⁶-DMSO) spectrum (δ ppm): 108.5, 118.8, 120.8, 123.6, 127.8, 128.9, 129.9, 131.6, 133.0, 133.7, 147.6, 158.1, 161.2, 162.2. Elemental Analysis C₄₂H₃₀N₆O₆ (714.72) (%) found C 70.34; H 4.48; N 12.02. calculated C 70.58; H 4.23; N 11.76.

3.2. Biological properties

3.2.1. Antimicrobial activity

Bacterial isolates used in this study were obtained from the Central Laboratories, Jordan Ministry of Health. The clinical isolates (*Escherichia coli*; *Klebsiella pneumoniae*; *Proteus mirabilis*; *Salmonella enteritidis*, *Pseudomonas aeruginosa*; *Staphylococcus aureus*; *Enterococcus faecalis*; *Bacillus cereus*) were grown in Muller Hinton Broth media for 24 h at 37 °C. The biological activity of the compounds was determined by establishing the minimum inhibitory concentration (MIC, mg/ μ L) using the micro-broth dilution method as described by Hannan [32]. Stock solutions of the compounds in DMSO were prepared according to CLSI guidelines [33]. The in vitro MIC was carried out in standard sterile 96 well flat bottom micro-titer plates. The layout was designed such that each row covered a range of concentrations from 500 to 0.5 mg/ μ L of the respective compounds under investigation with positive and negative control well. To each well, 40 μ L of the selected compounds at the correct concentration was added and the control well was loaded with a 40 μ L of DMSO solvent. Each well then received 150 μ L of Muller Hinton media and 10 μ L of the bacterial culture that was standardized with 0.5 McFarland turbidity standards. The final concentration of bacteria in the inoculum was approximately 5.0×10^7 CFU/ μ L. Plates were sealed and incubated at 37 °C under atmospheric conditions for 24 h. Micro-titer plates were read using an ELIZA UV–vis spectrometer. The minimal concentration that had an optical density below that of the control was defined as the MIC.

3.2.2. Antioxidant activity assays

The total antioxidant capacity of the tested hydrazones was measured spectrophotometrically by using the stable 1,1-diphenyl-2-picrylhydrazyl, 2,2'-azinobis(3-ethylbenzothiazoline-6-sulfonic acid)

free radicals in vitro assays. DPPH and ABTS have different mechanisms of neutralizing their free radical character. DPPH[•] absorbance decreases in presence of hydrogen-donating antioxidants due to the formation of the stable DPPH-H compound while ABTS is involved in an electron transfer process. Percent inhibition was calculated using Eq. (1):

$$\% \text{Inhibition} = \frac{\text{Absorbance of the control} - \text{absorbance of the tested sample}}{\text{Absorbance of the control}} \quad (1)$$

Then, the inhibition concentration 50 (IC₅₀) value was calculated based on a linear regression Eq. (2)

$$(y = ax + b) \quad (2)$$

from the curve by plotting the Ln concentration on x-axis and percentage of inhibition on y-axis.

3.2.3. DPPH scavenging activity assay

All synthesized compounds were screened for radical scavenging ability against DPPH (2,2-diphenyl-1-picrylhydrazyl) radical. A 1.0 mL of each test compound at different concentrations of (0.005, 0.01, 0.05, 0.10, 0.5 mg/mL) prepared in DMF was mixed with 1.0 mL of recently prepared solution of 0.10 mM DPPH in ethanol. The mixtures were stored in the dark for 30 min, and then, the absorbance of these solutions was obtained at ($\lambda = 517$ nm) using DMF solvent as a blank. Radical scavenging activity was determined according to the method of Blois [34]. The chemical response was compared with the one obtained under identical experimental conditions with ascorbic acid.

3.2.4. ABTS^{•+} scavenging activity assay

The total antioxidant capacity (TAC) in the ABTS assay was determined by the published methods [35, 36]. The ABTS assay utilizes the free mono-cation radical of 2,2'-azino-bis(3-ethylbenzothiazoline-6-sulfonic acid), generated by the oxidation of ABTS with potassium persulfate. The blue-green colored solution was dark stored for 1 day. The ABTS^{•+} cation radical solution was prepared by reacting of equivalent quantities of 7 mM of ABTS^{•+} and 2.4 mM of potassium persulfate (K₂S₂O₈) solution for 16 h at RT in the dark. Before using this solution, it was diluted with methanol to get an absorbance of 0.75 ± 0.02 at 734 nm. The reaction mixture was prepared by mixing 3.0 mL of ABTS^{•+} solution and 2.0 mL of tested compounds 3a-3 m at various concentrations (0.005, 0.01, 0.05, 0.10) mg/mL. The discoloration of the pre-generated ABTS^{•+} radical was measured at 734 nm and the chemical response was compared with the one obtained under identical experimental conditions with ascorbic acid.

3.3. Absorption and fluorescence spectroscopy

Absorption spectra of all compounds were recorded in DMSO using a Shimadzu UV-Vis absorption spectrometer Model UV 1800 in the spectral range 200–900 nm. The fluorescence spectra were recorded with an Edinburgh instruments fluorometer Model-FS 900SDT in the range 200–900 nm at room temperature. The photophysical studies of all compounds were performed in DMSO solutions, and the basic photophysical characteristics such as the absorption maxima (λ_{abs}) and emission maxima (λ_{em}) were determined.

3.4. Computational method

All electronic structure calculations were performed using the Wavefunction Spartan'18 Parallel Suite [37]. The structures of all prepared derivatives were fully optimized in the gas phase without any symmetry or geometry constraints at the B3LYP level of theory with the polarized 6-31G(d) basis set [38, 39, 40, 41, 42]. The lack of imaginary frequencies in the vibrational mode calculation verified that structures

were indeed true minima at the performed level of theory for each derivative.

4. Conclusions

Condensation of trimesic trihydrazide and aromatic aldehydes resulted in the formation of new series of hydrazone compounds. Spectral and elemental analysis were used to determine the structures of the synthesized hydrazone compounds. The optimized ground-state geometries of all prepared derivatives were elucidated using DFT calculations at the B3LYP/6-31G(d) level of theory. The results indicate that all structures feature trimeric propeller-shaped arrangements around a central 1,3,5-trisubstituted benzene. Their potential as antioxidants was studied using the DPPH and ABTS^{•+} scavenging activities. The **3g**, **3i** compounds showed highest DPPH radical scavenging ability. while, **3c**, **3l**, and **3m** were inactive toward DPPH assay. All test compounds exhibited good antioxidant capacity in the ABTS assay. Moreover, the inhibition activity of all hydrazones was found to be concentration dependent. Antimicrobial activity of the derivatives was estimated using a micro-broth dilution method. The MIC of all tested compounds were above 500 µg/mL and considered inactive.

Declarations

Author contribution statement

Ibrahim Mhaidat; Ayman Shdefat: Conceived and designed the experiments; Performed the experiments; Analyzed and interpreted the data; Contributed reagents, materials, analysis tools or data; Wrote the paper.

Fadel Alwedian; Taher Ababneh; Hasan Tashtoush: Analyzed and interpreted the data; Contributed reagents, materials, analysis tools or data; Wrote the paper.

Funding statement

This work was supported by the deanship of Scientific Research and Graduate Studies at Yarmouk University for providing the financial support of this work [project number 22/2016].

Data availability statement

The authors do not have permission to share data.

Declaration of interests statement

The authors declare no conflict of interest.

Additional information

No additional information is available for this paper.

Acknowledgements

The authors would like to thank the colleagues at chemistry department, Yarmouk University: Ayat Foudeh and Nourah Mhaidat for their help doing NMR and IR characterizations, special thanks to Zahra Smadi for her help doing the antioxidant measurements.

References

- H.S. Jois, B. Kalluraya, T. Vishwanath, Synthesis, spectroscopic properties and antioxidant activity of bis-hydrazones and schiff's bases derived from terephthalic dihydrazide, *J. Fluoresc.* 25 (3) (2015) 481–488.
- B. Smith Michael, J. March, *March's Advanced Organic Chemistry: Reactions, Mechanisms, and Structure*, John Wiley & Sons, 2007.
- G. Stork, J. Benaim, Monoalkylation of α , β -unsaturated ketones via metalloenamines: 1-butyl-10-methyl- $\Delta^{1(9)}$ -2-octalone, *Org. Synth.* 57 (1977) 69–73.
- R.M. Abdelhameed, O.M. Darwesh, M. El-Shahat, Synthesis of arylidene hydrazinylpyrido[2,3-d]pyrimidin-4-ones as potent anti-microbial agents, *Heliyon* 6 (2020), e04956.
- J.A. Sclafani, T.M. Maria, M.S. Thomas, A.V. Scott, Terminal alkylation of linear polyamines, *J. Org. Chem.* 61 (9) (1996) 3221–3222.
- D.R. Richardson, P.V. Bernhardt, Crystal, and molecular structure of 2-hydroxy-1-naphthaldehyde isonicotinoyl hydrazone (NIH) and its iron(III) complex: an iron chelator with anti-tumour activity, *J. Biol. Inorg. Chem.* 4 (3) (1999) 266–273.
- Y.S. Mallikarjun, A.P. Sangamesh, Synthesis, characterization, and biological studies of cobalt(II) and nickel(II) complexes with new Schiff bases, *Transit. Met. Chem.* 22 (3) (1997) 220–224.
- M. Katal, D. Yag, Analytical applications of hydrazones, *Talanta* 22 (2) (1975) 151–166.
- B.N. Ames, M.K. Shigenaga, T.M. Hagen, Oxidants, antioxidants, and the degenerative diseases of aging, *Proc. Nat. Acad. Sci. U. S. A.* 90 (17) (1993) 7915–7922.
- H. Sies, Oxidative stress: oxidants and antioxidants, *Exp. Physiol.* 82 (2) (1997) 291–295.
- Md. Nur Alam, N.J. Bristi, Md. Rafiquzzaman, Review on in vivo and in vitro methods evaluation of antioxidant activity, *Saudi Pharmaceut. J.* 21 (2) (2013) 143–152.
- D.W. Reische, D.A. Lillard, R.R. Eitenmiller, Antioxidants, in: C.C. Akoh, D.B. Min (Eds.), *Food Lipids Chemistry Nutrition and Biotechnology*, third ed., CRC Press, New York, NY, USA, 2008, pp. 409–433.
- P. Vicini, F. Zani, P. Cozzini, I. Doytchinova, Hydrazones of 1,2-benzisothiazole hydrazides: synthesis, antimicrobial activity and QSAR investigations, *Eur. J. Med. Chem.* 37 (7) (2002) 553–564.
- M.G. Mamolo, V. Falagiani, D. Zampieri, L. Vio, E. Banfi, Synthesis and antimycobacterial activity of [5-(pyridin-2-yl)-1,3,4-thiadiazol-2-ylthio]acetic acid arylidene-hydrazide derivatives, *Il Farmaco* 56 (8) (2001) 587–592.
- G.V.S. Kumar, Y. Rajendraprasad, B.P. Mallikarjuna, S.M. Chandrashekar, C. Kistayya, Synthesis of some novel 2-substituted-5-[isopropylthiazole] clubbed 1,2,4-triazole and 1,3,4-oxadiazoles as potential antimicrobial and antitubercular agents, *Eur. J. Med. Chem.* 45 (5) (2010) 2063–2074.
- E.J. Corey, D. Enders, Synthetic routes to polyfunctional molecules via metallated N,N-dimethylhydrazones, *Tetrahedron Lett.* 17 (1) (1976) 11–14.
- H. Shapiro Robert, *Organic Reactions. Alkenes from Tosylhydrazones*, John Wiley & Sons, 2011.
- P.C. Codruța, N.D. Hădăde, A.G. Coman, A. Gautier, F. Cisnetti, M. Matach, Symmetrical and non-symmetrical 2,5-diaryl-1,3,4-oxadiazoles: synthesis and photophysical properties, *Tetrahedron Lett.* 56 (25) (2015) 3961–3964.
- M.N. Arshad, A. Bibi, T. Mahmood, A.M. Asiri, K. Ayub, Synthesis, crystal structures and spectroscopic properties of triazine-based hydrazone derivatives, *Comparat. Experim. Theoret. Study Mol.* 20 (4) (2015) 5851–5874.
- A. Ali, M. Khalid, M. Abdul Rehman, F. Anwar, H. Zain-Ul-Aabidin, M.N. Akhtar, M.U. Khan, A.A. Carmo Braga, M.A. Assiri, M. Imran, An experimental and computational exploration on the electronic, spectroscopic, and reactivity properties of novel halo-functionalized hydrazones, *ACS Omega* 5 (30) (2020) 18907–18918.
- T. Kešić, D. Radanović, A. Pevec, I. Turel, M. Gruden, K. Anđelković, D. Mitić, M. Zlatar, B. Cobeljčić, Synthesis, X-ray structure and DFT calculation of magnetic properties of binuclear Ni(II) complex with tridentate hydrazone-based ligand, *J. Serb. Chem. Soc.* 85 (10) (2020) 1279–1290.
- N. Belkheiri, B. Bouguerne, F. Bedos-Belval, H. Duran, C. Bernis, R. Salvayre, A. Nègre-Salvayre, M. Baltas, Synthesis and antioxidant activity evaluation of a syringic hydrazones family, *Eur. J. Med. Chem.* 45 (2010) 3019–3026.
- H.S. Vidyashree Jois, Balakrishna Kalluraya, T. Vishwanath, Synthesis, spectroscopic properties and antioxidant activity of bis-hydrazones and schiff's bases derived from terephthalic dihydrazide, *J. Fluoresc.* 25 (2015) 1095–1102.
- N. Hristova-Avakumova, B. Nikolova-Mladenova, K. Yoncheva, V. Hadjimitova, Novel hydrazones – antioxidant potential and stabilization via polysaccharide particles, *J. Phys. Conf.* 780 (2017), 012004.
- A.D. Yılmaz, T. Coban, S. Suzen, Synthesis and antioxidant activity evaluations of melatonin based analogue indole-hydrazide/hydrazone derivatives, *J. Enzym. Inhib. Med. Chem.* 27 (3) (2012) 428–436.
- K. Velmurugan, D. Don, R. Kannan, C. Selvaraj, S. VishnuPriya, G. Selvaraj, S.K. Singh, R. Nandhakumar, Synthesis, antibacterial, antioxidant and molecular docking studies of imidazoquinolines, *Heliyon* 7 (7) (2021), e07484.
- I. Mhaidat, Z.A. Taha, W. Al Momani, A.K. Hijazi, Photoconductivity, antioxidant, and antimicrobial activities of some acenaphthenequinone derivatives, *Russ. J. Gen. Chem.* 89 (12) (2019) 2584–2590.
- Palani Elumalai, Palanisamy Rajakannu, Firasat Hussaina, Malaichamy Sathiyendiran, Design strategy for arranging an aromatic cyclic trimer into a tripodal molecule, *RSC Adv.* 3 (2013) 2171–2173.
- S. Kumar, A. Das, Mimicking trimeric interactions in the aromatic side chains of the proteins: a gas phase study of indole...(pyrrole)₂ heterotrimer, *J. Chem. Phys.* 136 (2012) 174302.
- M. Sathiyendiran, J.Y. Wu, M. Velayudam, G.H. Lee, S.M. Peng, K.L. Lu, Neutral metallacyclic rotors, *Chem. Commun.* (2009) 3795–3797.
- L. Yang, L. Zhihua, H. Cheng, Z. Liang, D. Chunying, A symmetry-controlled and face-driven approach for the assembly of cerium-based molecular polyhedral, *Dalton Trans.* 39 (2010) 11122–11125.

- [32] C.T. Hannan Peter, Guidelines and recommendations for antimicrobial minimum inhibitory concentration (MIC) testing against veterinary mycoplasma species, *Vet. Res.* 31 (4) (2000) 373–395.
- [33] P.A. Wayne, Clinical and Laboratory Standards Institute (CLSI) Performance Standards for Antimicrobial Disk Diffusion Susceptibility Tests 19th Ed. Approved Standard, 2009. CLSI document M100-S19 29.
- [34] M.S. Blois, Antioxidant determinations using a stable free radical, *Nature* 181 (1958) 1199–1200.
- [35] R. Re, N. Pellegrini, A. Proteggente, Antioxidant activity applying an improved ABTS radical cation decolorization assay, *Free Radic. Biol. Med.* 26 (9-10) (1999) 1231–1237.
- [36] M.A. Al-Qudah, S.M. Obeidat, R. Mhaidat, B. Al-Trad, H.I. AlJaber, J.N. Lahham, Intercomparative investigation of the total phenols, total flavonoids, in vitro and in vivo antioxidant activities of *Capparis Cartilaginea* (Decne.) maire and weiller and *Capparis Ovata* Desf. from Jordan, *Phcog. Mag.* 14 (55) (2018) 154.
- [37] Spartan software, Wavefunction inc., irvine, CA.
- [38] D. Becke, Density-functional thermochemistry. III. The role of exact exchange, *J. Chem. Phys.* 98 (1993) 5648–5652.
- [39] A.D. Becke, Density-functional thermochemistry. IV. A new dynamical correlation functional and implications for exact-exchange mixing, *J. Chem. Phys.* 104 (1996) 1040–1046.
- [40] C. Lee, W. Yang, R.G. Parr, Development of the Colle-Salvetti correlation-energy formula into a functional of the electron density, *Phys. Rev. B* 37 (1988) 785–789.
- [41] G.A. Petersson, A. Bennett, T.G. Tensfeldt, M.A. Al-Laham, W.A. Shirley, J.A. Mantzaris, A complete basis set model chemistry. I. The total energies of closed-shell atoms and hydrides of the first-row elements, *J. Chem. Phys.* 89 (1988) 2193–2218.
- [42] G.A. Petersson, T.G. Tensfeldt, J.A. Montgomery Jr., A complete basis set model chemistry. III. The complete basis set-quadratic configuration interaction family of methods, *J. Chem. Phys.* 94 (1991) 6091–6101.